# Two-dimensional correlation spectroscopic analysis on the interaction between humic acids and aluminum coagulant

Pengkang Jin[1,*], Jina Song[1,2], Xiaochang C. Wang[1], Xin Jin[1]

1. School of Environmental and Municipal Engineering, Xi'an University of Architecture and Technology, Xi'an 710055, China
2. College of Energy and Environmental Engineering, Hebei University of Engineering, Handan 056038, China

## ARTICLE INFO

## ABSTRACT

In this study, two-dimensional correlation spectroscopy integrated with synchronous fluorescence and infrared absorption spectroscopy was employed to investigate the interaction between humic acids and aluminum coagulant at slightly acidic and neutral pH. Higher fluorescence quenching was produced for fulvic-like and humic-like fractions at pH 5. At pH 5, the humic-like fractions originating from the carboxylic acid, carboxyl and polysaccharide compounds were bound to aluminum first, followed by the fulvic-like fractions originating from the carboxyl and polysaccharide compounds. This finding also demonstrated that the activated functional groups of HA were involved in forming the Al-HA complex, which was accompanied by the removal of other groups by co-precipitation. Meanwhile, at pH 7, almost no fluorescence quenching occurred, and surface complexation was observed to occur, in which the activated functional groups were absorbed on the amorphous $Al(OH)_3$. Two-dimensional FT-IR correlation spectroscopy indicated the sequence of HA structural change during coagulation with aluminum, with IR bands affected in the order of $COOH > COO^- > NH$ deformation of amide II > aliphatic hydroxyl $C-OH$ at pH 5, and $COO^- >$ aliphatic hydroxyl $C-OH$ at pH 7. This study provides a promising pathway for analysis and insight into the priority of functional groups in the interaction between organic matters and metal coagulants.

## Introduction

Humic acid (HA) is the major component of natural organic matter (NOM) and is responsible for the formation of harmful disinfection by-products (DBPs). Currently, the removal of HA from natural waters is primarily achieved using chemical coagulation/flocculation followed by sedimentation or flotation (Wang et al., 2014). Aluminum salts have been extensively used as coagulants because of the strong ability of the cationic hydrolytic species to remove small particles and HA moieties (Zhou and Meng, 2016).

The ability of HA to interact with aluminum salts is attributed to its high content of oxygen-containing functional groups, such as carboxyl, hydroxyl, and carbonyl (Provenzano et al., 2004). A number of analytical techniques are available to study the interaction mechanisms between HA and aluminum coagulants, which include fluorescence quenching, fluorescence excitation-emission matrix spectroscopy (EEMs), X-ray photoelectron spectroscopy (XPS), nuclear magnetic resonance (NMR), Fourier transform infrared (FT-IR) and high-performance size-exclusion chromatography (HPSEC) (Cheng and Chi, 2002; Hussain et al., 2013; Lin et al., 2014; Lu et al., 1999; Zhu et al.,

---

2014). These methods have provided insight into the interaction mechanisms between HA and aluminum coagulants based on distinct fluorescence quenching behavior, Al species in the Al-HA flocs, the structures and functionalities of complexes, *etc.* However, it is well known that HA is a macromolecular organic substance with a complex and difficult-to-identify structure. The coagulation effect is attributed to its high content of oxygen-containing functional groups (Cheng and Chi, 2002). Moreover, the coagulation characteristics of the coagulant and various functional groups of HA are distinctive because of the distinct polarity, dissociation and reaction rates of the functional groups. Accordingly, it is necessary to describe the priority of functional groups in the interaction between humic acids and aluminum coagulants. However, it is difficult to identify the sequence of functional groups in HA reacting with the Al coagulant through these methods.

In 1986, Noda proposed the use of the two-dimensional correlation spectroscopy (2D-COS) method to analyze a set of spectral data from a system under the influence of an external perturbation (Noda, 1986), which introduced a new method in the investigation of binding ability between metal ions and organic ligands. Soon afterward, 2D-COS was increasingly applied in various studies. Recent research has explored the binding of natural organic matter (NOM) with metal cations such as $Cu^{2+}$, $Pb^{2+}$ and $Zn^{2+}$ (Chen et al., 2015; Hur and Lee, 2011; Nakashima et al., 2008; Xu et al., 2013), or the binding of organic ligands in dissolved organic matter from soil with $Al^{3+}$ to understand soil organic carbon storage (Yu et al., 2012) by using 2D-COS. These studies have revealed distinct binding behaviors and the distribution of the binding sites with different metal and organic matter fractions. However, compared with other metal ions, aluminum not only can act as a coagulant that forms a complex with HA followed by the formation of flocs, but also is capable of absorbing HA on the surface of $Al(OH)_{3(s)}$. Therefore, although 2D-COS has been used for the characterization of metal–organic complexes, the characteristics of coagulation of humic acids by aluminum coagulants are quite different from the previous studies on metal–organic complexes, and the distinctive removal rules of functional groups during the coagulation of HA still remain poorly understood.

In principle, two-dimensional correlation spectroscopy could resolve the overlapped peaks and enhance the spectral resolution by extending the spectral intensity within the data, collected as a function of an external perturbation (*e.g.*, time, temperature and concentration), along the second dimension. More importantly, the specific sequential orders of the spectral intensity changes, *i.e.*, structural variations, can be probed through synchronous and asynchronous spectral analysis (Yu et al., 2012), which may be useful to investigate the sequence in which the functional groups in HA react with Al. Moreover, 2D heterospectral correlation spectroscopy could investigate the covariation of two different spectra, such as FT-IR and synchronous fluorescence (He et al., 2014). This approach may be used to identify the functional groups that are responsible for the peaks in the synchronous fluorescence spectra. Therefore, aiming to probe the characteristics and the sequential order of the corresponding functional groups of HA removed by coagulation, the structural changes of HA as a function of aluminum coagulant concentration were examined using synchronous fluorescence and FT-IR spectroscopy coupled with 2D-COS analysis. Thus, this study provides a promising pathway to analyze the priority of functional groups in the interaction between HA and aluminum coagulants.

## 1. Materials and methods

### 1.1. Materials and reagents

Humic acid was obtained from Sigma-Aldrich. The stock HA solution was prepared by adding 1 g of HA into 1 L of 0.1 mol/L NaOH solution. After stirring for 12 hr, the samples were filtered through a 0.45-$\mu$m membrane to remove the suspended materials and then passed through $H^+$-saturated AG-MP 50 cation exchange resin (Bio-Rad) in the hydrogen-saturated form. The resin was packed in 20 mm ID × 300 mm L glass columns and rinsed with 0.1 mol/L NaOH, 0.1 mol/L HCl and deionized water just prior to the extraction. Finally, the hydrogen-saturated acids were adjusted to different pH levels and then lyophilized for the FT-IR analyses.

### 1.2. Jar test procedure

Coagulation studies were performed in a conventional jar-test apparatus, equipped with six 1-L beakers. The stock HA solution was diluted with ionized water to reach the designated concentration (DOC = 10 mg/L). In addition, $NaNO_3$ was added to adjust the ionic strength of the solution to 0.1 mmol/L. Aluminum chloride (41.4 mmol/L $Al^{3+}$) was used in the study. The calculated volume of coagulation stock solution (to achieve the required dosage) and NaOH solution (to achieve the required pH) was added to the HA (DOC = 10 mg/L) solution. The coagulation procedure involved rapid mixing at 200 r/min for 1 min, followed by slow stirring at 20 r/min for 30 min. Approximately 20 mL of the solution was taken to determine the fluorescence intensity of the coagulating suspension within 1 min after flocculation. A 60-min settling period followed. The precipitate was then separated from the solution by centrifugation at 6000 r/min for 10 min and later lyophilized for FT-IR analyses.

### 1.3. Synchronous fluorescence spectra

Synchronous fluorescence spectra were recorded using an FP-6500 fluorescence spectrophotometer (Jasco, Japan). The excitation and emission slits were both adjusted to 5 nm, and the excitation wavelengths ranging from 250 to 550 nm were used with a constant offset ($\Delta\lambda = 30$ nm).

### 1.4. FT-IR analysis

A mixture of 0.5 mg sample and 50 mg of KBr was ground and then compressed. The pellets were analyzed using a Fourier transform infrared (FT-IR) spectrometer (Model Nicolet 6700, Thermo Fisher Scientific) covering a frequency range of 4000–500 $cm^{-1}$.

### 1.5. Two-dimensional correlation spectroscopy

The 2D correlation spectra were produced according to the method of Noda and Ozaki (2004). Fig. 1 shows the general

procedure for a 2D correlation spectroscopy experiment. In typical one-dimensional spectroscopy, a selected electromagnetic probe is used by itself to study the system of interest. The interaction between the probe and system constituents is then recorded as a spectrum. In 2D correlation spectroscopy, the system is additionally placed under the influence of some external perturbation (such as time, temperature, pH, concentration, *etc.*), which in turn induces changes in the spectral features. Such spectral variations are traditionally referred to as dynamic spectra. In a typical 2D experiment, a series of perturbation-induced dynamic spectra are collected in some sequential order. Then a computational method is used to generate a pair of correlation intensity maps, *i.e.*, synchronous and asynchronous correlation spectra (Noda, 2012).

Synchronous spectra consist of autopeaks located along the main diagonal of the map and cross-peaks located at the off-diagonal positions. Autopeaks represent the overall susceptibility of the corresponding spectral region to change in spectral intensity as an external perturbation is applied to the system. Cross-peaks indicate simultaneous changes of spectral intensities observed at two different spectral variables $v_1$ and $v_2$. A positive cross-peak indicates that the intensity changes at the corresponding spectral coordinates are either increasing or decreasing together, while a negative value suggests the opposite direction. Asynchronous spectra show cross-peaks exclusively. The signs of cross-peaks in synchronous and asynchronous spectra provide the sequential order of spectral intensity variations along the external variable (Hur et al., 2011). Based on Noda's rules, if the signs of the synchronous and asynchronous cross-peaks are the same below the diagonal line, then the change in the spectral intensity at the $v_1$ band occurs before the $v_2$ band. This order is reversed when the signs are different. The spectral intensity at $v_1$ and $v_2$ changes simultaneously if the sign of asynchronous spectra is zero (Chen et al., 2014).

In this study, the aluminum coagulant concentration was applied as an external perturbation, and a set of concentration-dependent synchronous fluorescence and FT-IR spectra was obtained. All calculations were performed using 2D Shige software (Kwansei-Gakuin University, Japan). Synchronous and asynchronous spectra were plotted using Origin software.

## 2. Results and discussion

### 2.1. Changes in the synchronous fluorescence spectra of HA with aluminum coagulant

The coagulation pH is the most significant treatment parameter affecting the humic acid removal by coagulation. The optimal pH range for the coagulation of HA has been found to be 5 (Semmens and Field, 1980). In general, coagulation experiments are conducted at neutral pH, which is also effective in removing HA at the expense of higher doses of coagulant. To compare the interaction behaviors under neutral conditions (commonly used in water treatment) and the optimum pH, two pH values (pH 5.0 and pH 7.0) were selected.

Changes in the synchronous fluorescence spectra of HA upon the addition of $Al^{3+}$ at pH 5.0 and pH 7.0 are shown in Fig. 2. At such concentration range of aluminum, no $Al(OH)_{3(s)}$ formed. Three fluorescence regions at the wavelength of 250 to 300, 300 to 380, and 380 to 550 nm were assigned to protein-like, fulvic-like, and humic-like fluorescence fractions, respectively (Chen et al., 2015). Synchronous fluorescence spectra of the initial HA at pH 5.0 and pH 7.0 exhibited two prominent peaks at 370 nm and 440 nm, which were related to fulvic-like and humic-like fluorescence fractions, respectively. The fluorescence intensity of protein-like fractions was relatively low, compared with that of the fulvic-like and humic-like fractions.

Upon ultraviolet (UV) excitation, the unsaturated components could emit fluorescence (Cheng and Chi, 2002). If HA forms complexes with metal salts, the fluorescence would be either enhanced or quenched (Sharpless and Mcgown, 1999; Elkins and Nelson, 2002). A decrease in the fluorescence intensity was detected after the addition of aluminum, which indicated fluorescence quenching by metal–organic ligand complexation (Sharpless and Mcgown, 1999; Elkins and Nelson, 2002). At pH 5, with increasing aluminum concentration, fluorescence quenching occurred for fulvic-like and humic-like fractions, indicating complex formation between HA and aluminum, whereas little change occurred for the protein-like fractions. The degree of fluorescence quenching at pH 5 was more pronounced. For example, 43% and 64.6% of the initial
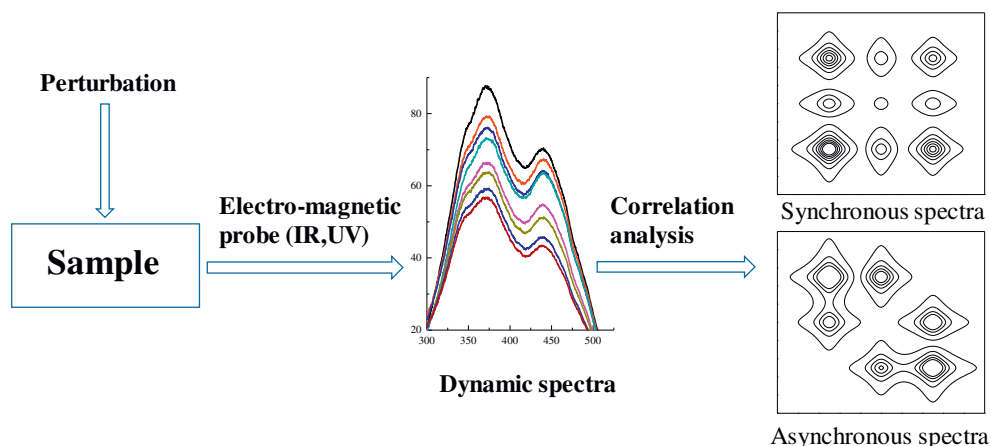


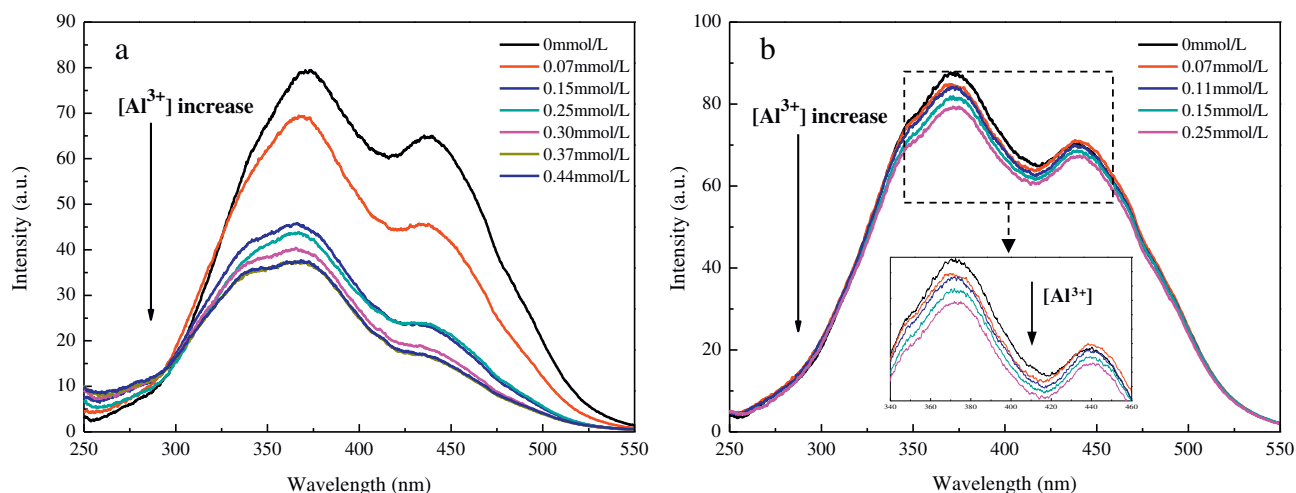**Fig. 1 – General procedure for 2D correlation spectroscopy.**

**Fig. 2 – Changes in the synchronous fluorescence spectra of humic acids upon addition of aluminum at pH 5.0 (a) and 7.0 (b).**

fulvic-like and humic-like fluorescence peak intensities, respectively, were reduced with 0.15 mmol/L $Al^{3+}$ dosage. The degree of quenching for fulvic-like and humic-like fractions was not the same, suggesting that the different fractions of HA had varying affinities to aluminum.

Such different fluorescence quenching behavior was less pronounced at pH 7, with only 6.7% and 2.7% of the initial fulvic-like and humic-like fluorescence peak intensities, respectively, reduced with 0.15 mmol/L $Al^{3+}$ dosage. The results indicated that less HA may be involved in complexation with aluminum, which could be related to the coagulation characteristics at pH 7. Our previous studies found that HA coagulation *via* adsorption rather than complexation did not occur until the coagulant dosage became high enough to form aluminum hydroxide at pH ≥ 7 (Jin et al., 2011).

### 2.2. FT-IR spectroscopic analysis on coagulation of HA

The infrared spectra of HA at pH 3, 5 and 7 are shown in Fig. 3. The fully protonated HA was characterized by absorption bands at pH 3. Major absorption bands at pH 3 occurred at 3110 $cm^{-1}$(C–H in aromatic structures), 1717 $cm^{-1}$ (C=O stretching of COOH), 1608 $cm^{-1}$ (aromatic C=C, strongly H-bonded C=O, C=C conjugated with C=O, or a combination of these), 1400 $cm^{-1}$ (C–H deformation of aliphatic groups), 1247 $cm^{-1}$ (C–O stretching and OH deformation of COOH), and 1000–1100 $cm^{-1}$ (OH deformation and C–O stretching of phenolic and alcoholic OH groups) (Piccolo and Stevenson, 1982).

Many studies have showed that the carboxyl group of HA plays an important role in coagulation and that coagulation could be affected by the deprotonation of carboxyl groups with increasing pH (Angelico et al., 2014; Alvarez-Puebla and Garrido, 2005). A considerable amount of free carboxylic groups was found to exist at pH 3, as evidenced by bands at 1717 $cm^{-1}$ and 1247 $cm^{-1}$. With an increase of the pH value, the amount of free carboxylic groups decreased, and the conversion of COOH to COO⁻ led to the expected loss of absorption at 1717 $cm^{-1}$ and 1247 $cm^{-1}$ at pH 5, as well as its complete loss at pH 7. Deprotonation of COOH was

accompanied by the appearance of characteristic bands caused by asymmetric and symmetric stretching of COO⁻ near 1594 $cm^{-1}$ and 1389 $cm^{-1}$ at pH 5, respectively. At complete deprotonation at pH 7, the absorption in these regions was centered at 1578 $cm^{-1}$ and 1388 $cm^{-1}$ for asymmetric and symmetric stretching of COO⁻, respectively.

The infrared spectra of HA at pH 5 before and after coagulation are shown in Fig. 4a. The absorption band at 1247 $cm^{-1}$ disappeared, and the intensity of the 1717 $cm^{-1}$ band diminished with increasing aluminum dosage. In addition, the bands at 1600 $cm^{-1}$ and 1390 $cm^{-1}$ shifted to higher frequency at different coagulant dosages, suggesting the formation of complexes between HA and aluminum. Piccolo and Stevenson (1982) showed similar results in the investigation of complexes of $Cu^{2+}$ with humic acids. They reported that the antisymmetric COO⁻ band shifted from 1610 to 1625 $cm^{-1}$, and the symmetric COO⁻ band centered at 1400 $cm^{-1}$ shifted to
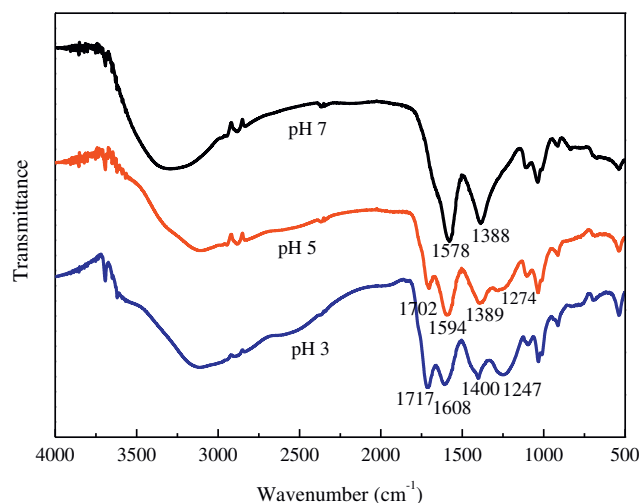


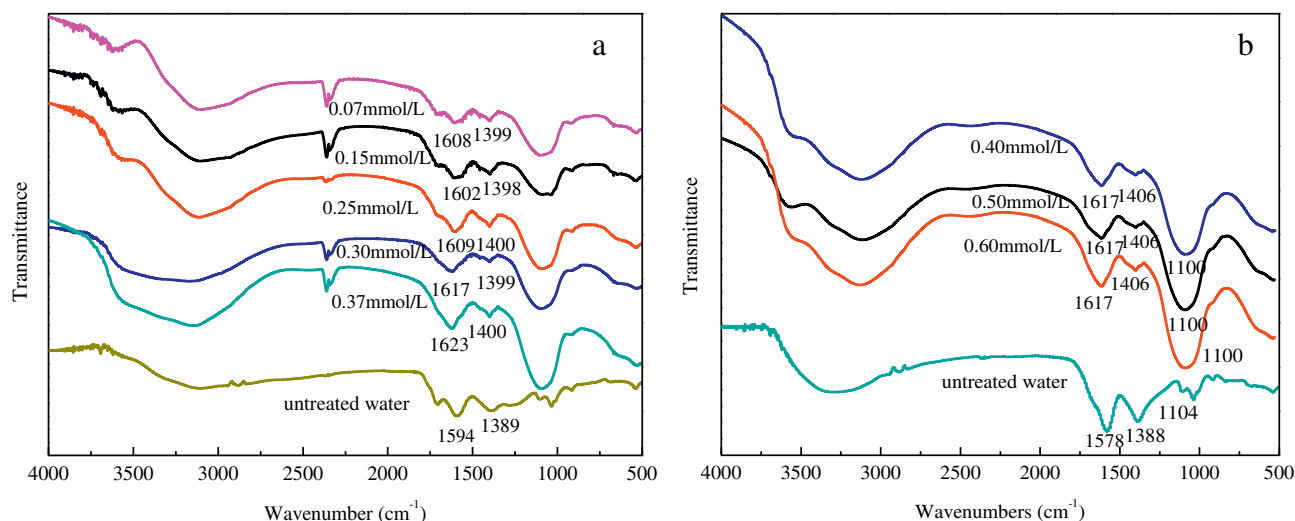**Fig. 3 – Fourier transform infrared of HA at different pH values.**

**Fig. 4 – FT-IR spectra of humic acid after coagulation at pH 5 (a) and 7 (b).**

1390 cm$^{-1}$ for the Cu$^{2+}$-humic complexes. The lone pair electrons of oxygen atoms from the hydroxyl in carboxyl could conjugate with the π-bond of carbonyl. The competition for the lone pair electrons between aluminum and carbonyl caused by the addition of aluminum reduces the polarity of carbonyl, consequently enhancing the bond energy; as a result, the required energy to excite electrons increases, thereby increasing the frequency.

The infrared spectra of HA at pH 7 before and after coagulation are shown in Fig. 4b. As we all know, the dominant coagulation mechanism is adsorption of organic species on amorphous Al(OH)$_3$ at pH 7. Adsorption occurred by surface complexation with activated groups of HA molecules on Al(OH)$_{3(s)}$ (Shin and Spinette, 2008). The surface complexation reactions have been described as inner-sphere and outer-sphere complexes. In the infrared spectra, little or no band shift is expected for outer-sphere surface complexes, and band shifts to higher wavenumbers are expected for inner-sphere surface complexes (Nordin et al., 1997). As shown in Fig. 4b, the antisymmetric COO$^-$ band shifted from 1578 cm$^{-1}$ to 1617 cm$^{-1}$, and the symmetric COO$^-$ band centered at 1388 cm$^{-1}$ shifted to 1406 cm$^{-1}$ for all aluminum dosages. The aliphatic hydroxyl C–OH band shifted from 1104 cm$^{-1}$ to 1100 cm$^{-1}$. These pieces of evidence revealed the formation of inner-sphere surface complexes to carboxyl and outer-sphere surface complexes to aliphatic hydroxyl at the aluminum hydroxide surface. For Al(OH)$_{3(s)}$ adsorption, the carboxylic group on a humic molecule is first complexed to the Al nuclei on the surface of Al(OH)$_3$; next, further progressive adsorption of the rest of the molecule on the surface of Al(OH)$_3$ occurs *via* physical and chemical forces, such as van der Waals forces and H-bonding (Lu et al., 1999). Similar trends were observed by Guan et al. (2006) in the study of the interaction between NOM and aluminum hydroxide. They found that both the asymmetric and symmetric vibrations of the carboxylate group shifted to higher frequency upon adsorption of 3,5-dihydroxybenzoic acid, indicating that the carboxyl group complexed with Al$^{3+}$ on the adsorbent surface.

### 2.3. Two-dimensional FT-IR correlation analysis on coagulation of HA at pH 5 and pH 7

To understand the sequence of HA functional group binding to Al with increasing aluminum dosage at pH 5 and 7, a two-dimensional correlation analysis was performed (Fig. 5). The 1750–950 cm$^{-1}$ region of 2D FT-IR correlation spectra was primarily analyzed because this spectral region includes the bands corresponding to amides, carboxylic acids, esters, aliphatic groups and carbohydrates (Li et al., 2014).

Fig. 5a shows the synchronous and asynchronous spectra generated from the FTIR spectra with the aluminum dosage from 0.07 to 0.37 mmol/L (no Al(OH)$_3$ formation) at pH 5.0. Four autopeaks centered at 1715, 1562, 1406 and 1104 cm$^{-1}$ were displayed in the synchronous spectra. The band at 1104 cm$^{-1}$ was shown to change most significantly, followed by bands at 1562 and 1406 cm$^{-1}$. The smallest change was observed for the band at 1715 cm$^{-1}$. The signs of the cross-peaks in the synchronous map were all positive, except for those associated with the 1104 cm$^{-1}$ band. This result indicated that the conformational changes associated with most IR bands were in the same direction, whereas those associated with the 1104 cm$^{-1}$ band were in the reverse direction. In the asynchronous map, the band at 1610 cm$^{-1}$ that overlapped in the synchronous spectra could be identified from the cross-peaks. The bands were assigned as follows: the band at 1715 cm$^{-1}$ corresponds to the C=O stretching of COOH, the bands at 1610 cm$^{-1}$ and 1406 cm$^{-1}$ correspond to the asymmetric and symmetric stretching of COO$^-$, the band at 1562 cm$^{-1}$ corresponds to the NH deformation of amide II, and the band at 1104 cm$^{-1}$ corresponds to the C–OH stretching of aliphatic OH groups. The signs of their cross-peaks in the synchronous ($\Phi(v_1,v_2)$) and asynchronous ($\Psi(v_1,v_2)$) spectra are shown in Table 1. Using Noda's rule, the sequence of HA structural change in coagulation with aluminum at pH 5 followed the order: 1715 cm$^{-1}$ (carboxylic acid C=O) → 1610 cm$^{-1}$, 1406 cm$^{-1}$ (COO$^-$) → 1562 cm$^{-1}$ (NH deformation of amide II) → 1104 cm$^{-1}$ (aliphatic hydroxyl C–OH).
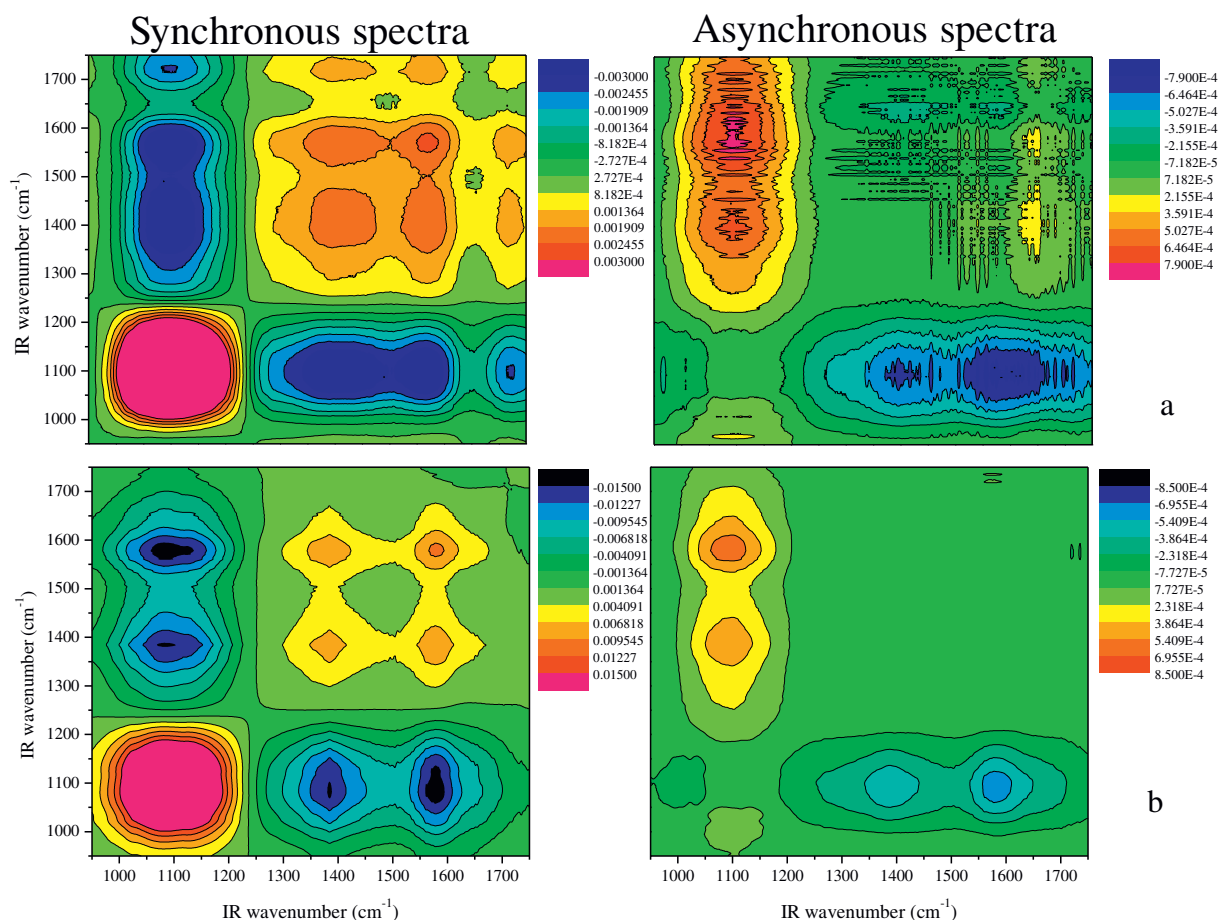
## Synchronous spectra

## Asynchronous spectra



**Fig. 5 – Synchronous and asynchronous 2D correlation spectra of HA after coagulation (a: at pH 5.0; b: at pH 7.0) in the region of 1750–950 cm$^{-1}$.**

Fig. 5b shows the synchronous and asynchronous spectra generated from the FT-IR spectra with the aluminum dosage at pH 7.0. In the synchronous spectra three major autopeaks centered at 1100, 1390 and 1582 cm$^{-1}$ were revealed. The bands were attributed as follows: the bands at 1582 cm$^{-1}$ and 1390 cm$^{-1}$ correspond to the asymmetric and symmetric stretching of COO$^{-}$, and the band at 1100 cm$^{-1}$ corresponds to the C–OH stretching of aliphatic OH groups. The change in band intensity followed the order: 1100 cm$^{-1}$ > 1582 cm$^{-1}$ > 1390 cm$^{-1}$; as a result, the susceptibility (or change degree) of

HA with aluminum dosage has the following order: aliphatic hydroxyl C–OH>COO$^{-}$. Using the sequential order rules, it could be concluded that the structural change sequence of HA backbones in coagulation with aluminum followed the order: 1390, 1582 cm$^{-1}$ (COO$^{-}$) > 1065 cm$^{-1}$ (aliphatic hydroxyl C–OH).

### 2.4. Two-dimensional fluorescence spectroscopy correlation analysis

As discussed above, almost no fluorescence quenching occurred at pH 7, confirming that the fluorescence intensity was independent of the aluminum coagulant concentration. Therefore, only 2D-COS at pH 5 will be considered in the following sections.

The synchronous maps at pH 5 showed two autopeaks centered at 370 nm and 440 nm corresponding to fulvic-like and humic-like fluorescence fractions (Fig. 6a). The intensities of the peaks decreased in the order 440 nm and 370 nm at pH 5, suggesting that the fluorescence of humic-like fractions was more susceptible to aluminum addition. All the cross peaks were positive, because both of the bands at 370 nm and 440 nm had decreasing intensities with increasing aluminum concentration.

The asynchronous map revealed the sequential changes of fluorescence fractions with addition of aluminum coagulant.

**Table 1 – Sign of each cross-peak in the synchronous (Φ) and asynchronous (Ψ, in brackets) maps from the IR spectra after coagulation at pH 5.**

| Position (cm$^{-1}$) | Sign | | | | |
|---|---|---|---|---|---|
| | 1104 | 1406 | 1562 | 1610 | 1715 |
| 1104 | + | −(+) | −(+) | −(+) | −(+) |
| 1406 | | + | +(+) | +(/) | +(−) |
| 1562 | | | + | +(−) | +(+) |
| 1610 | | | | + | +(−) |
| 1715 | | | | | + |

Signs were obtained in the lower right corner of the maps, + positive, − negative, / no cross-peak.
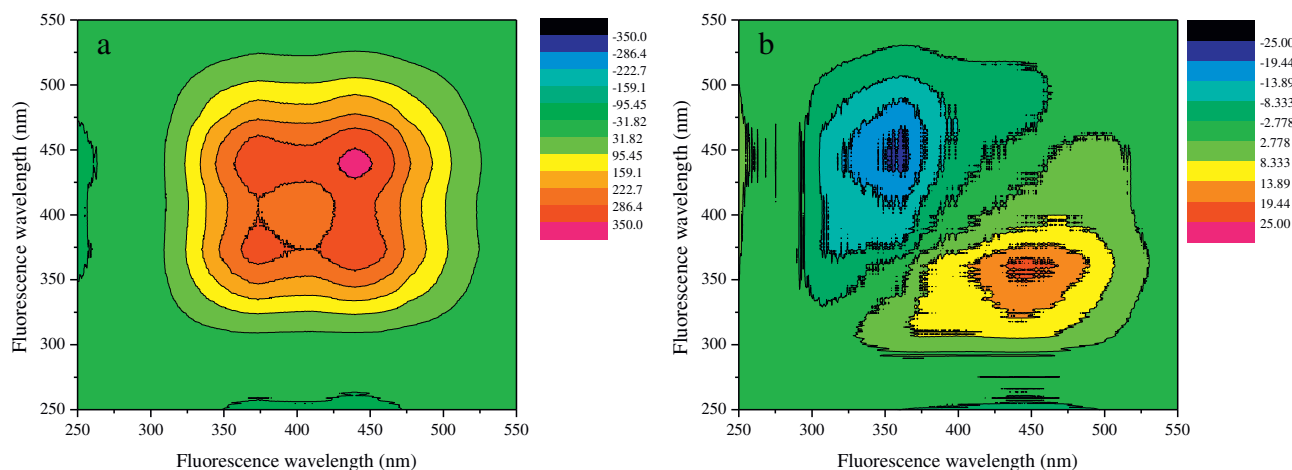
**Fig. 6 – Synchronous (a) and asynchronous (b) 2D correlation maps generated from the synchronous fluorescence spectra of HA with increasing aluminum dosage at pH 5.**

As shown in Fig. 6b, a negative cross peak was shown at $v_1/v_2$ of 370/440 nm below the diagonal line of the asynchronous 2D fluorescence correlation spectrum at pH 5. By comparing the sign of the cross peak in the synchronous and asynchronous maps, we can extract information about the change, which followed the order 440 nm > 370 nm according to Noda's rule. This result suggested that aluminum coagulant bound to HA fractions in the following sequence: humic-like fraction → fulvic-like fraction at pH 5.

### 2.5. Two-dimensional fluorescence/IR spectroscopy hetero-correlation analysis

Two-dimensional heterospectral correlation spectroscopy is used to examine covariations between two types of spectra. A positive correlation suggests the existence of a coupled or related origin of the spectral intensity variations detected in the two spectra (He et al., 2014). The 2D FT-IR-fluorescence hetero-correlation spectroscopy showed that the fluorescence band at 440 nm was positively correlated with the FT-IR bands at 1402 and 1581 $cm^{-1}$ ($COO^-$), 1712 $cm^{-1}$ (COOH), and 1000 $cm^{-1}$ (polysaccharides $C-O$) (Fig. 7), which indicates that the humic-like fraction originated from the carboxylic acid, carboxyl and polysaccharide compounds. In addition, the fluorescence band at 370 nm showed a positive correlation with the FT-IR bands at 1402 and 1581 $cm^{-1}$ and at 1000 $cm^{-1}$. This result suggests that the fulvic-like fraction originated from the carboxyl and polysaccharide compounds.

### 2.6. Mechanism analysis

Based on the above analysis, the mechanism of the interaction of humic acid with aluminum coagulants can be interpreted as shown in Fig. 8. As is known, HA comprises a complex, heterogeneous group of macromolecules with various functional groups, which determine its chemical properties. The pH value is one of the important variables that affects the surface charge of HA because of the protonation/deprotonation of the oxygen-containing functional groups. The predominant functional groups of HA contain carboxylic and phenolic groups. It is

believed that the pKa values of 4–6 correspond approximately to those of carboxylic acids, and a pKa value of 10 corresponds to those of the phenolic functional groups (Zhou et al., 2005). At pH 5, carboxylic groups can be protonated, thus allowing HA to react with aluminum. As indicated in the fluorescence and FT-IR analysis, the carboxylic groups on HA formed complexes with aluminum. These functional groups react with metal coagulant via $OH^-$ in water as the medium to form a metal-HA complex. Under this condition, unlike colloidal particles, the coagulation of humic acid underwent a transition from dissolved form to insoluble particles. The phase transition from the dissolved state to the solid state occurred by the complexation of metal salts with HA molecules to form insoluble particles. Afterwards, these insoluble particles collided with each other to form large aggregates. Therefore, co-precipitation could occur after the active groups form the Al-HA complex, which resulted in the removal of other groups, such as carboxylic acid, NH of amide II and aliphatic hydroxyl.

At pH 7, the fluorescence quenching behavior was less pronounced, indicating that less HA may be involved in
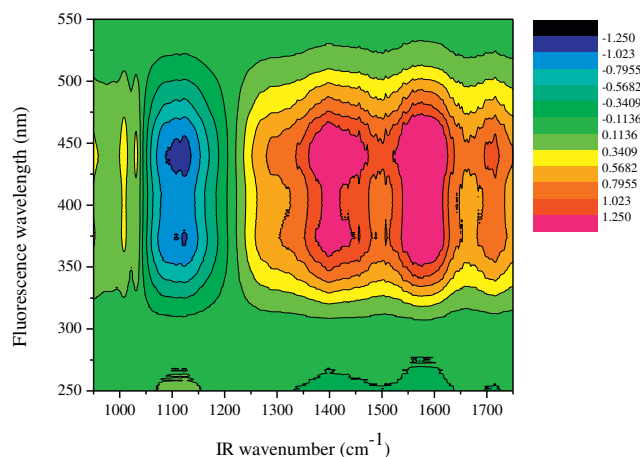


**Fig. 7 – 2D FT-IR-fluorescence heterospectral correlation spectrum of HA after coagulation at pH 5.**
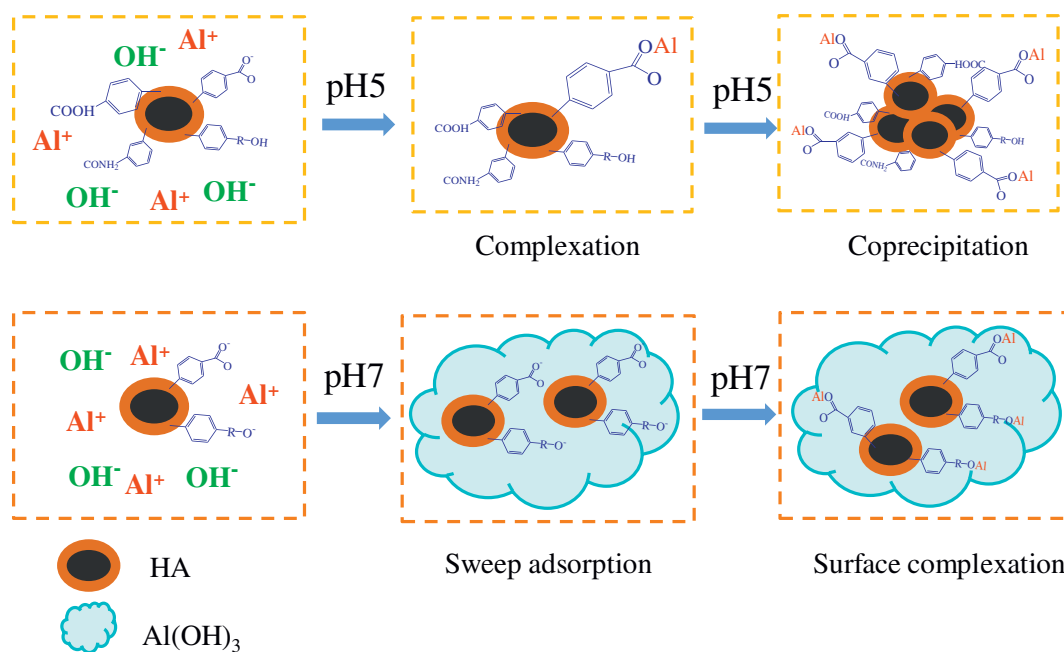
**Fig. 8 – Mechanism of interaction of humic acid with aluminum coagulants.**

complexation with aluminum. Aluminum hydrolysis mainly occurs to form aluminum hydroxide, $Al(OH)_{3(s)}$. Therefore, adsorption onto $Al(OH)_{3(s)}$ is a primary pathway for the removal of HA. Adsorption occurs by surface complexation of HA molecules with surface groups on $Al(OH)_{3(s)}$ (Shin and Spinette, 2008). The carboxyl groups adsorbed to the $Al(OH)_{3(s)}$ surface and formed inner-sphere surface complexes. A small amount of aliphatic hydroxyl groups could also be ionized and formed outer-sphere surface complexes at the aluminum hydroxide surface.

## 3. Conclusions

The HA and aluminum coagulant interactions at pH 5 and pH 7 were studied by the use of synchronous fluorescence, FT-IR and 2D-correlation analysis. Two types of reaction patterns in the coagulation of HA by Al were proposed. Carboxyl was found to play an important role in binding to aluminum to form the Al-HA complex, which resulted in the occurrence of co-precipitation for the removal of HA in water at pH 5. In addition, carboxyl and aliphatic hydroxyl participated in surface complexation on the surface of amorphous $Al(OH)_3$ at pH 7. Two-dimensional FTIR correlation spectroscopy further revealed the preferential removal of carboxylic acid and carboxyl groups, as well as the delayed response of IR bands from NH deformation of amide II and aliphatic hydroxyl at pH 5; at pH 7, the carboxyl group provided the fastest responses followed by the aliphatic hydroxyl group. These findings demonstrated that the application of 2D correlation spectroscopic analysis can provide insight into the priority of the functional groups in the interaction between humic acids and aluminum coagulants. Knowledge of how the pH value influences the sequence of the interactions of aluminum coagulant to different chemical groups of HA will help to better understand the coagulation characteristics at different pH levels.

## R E F E R E N C E S

Alvarez-Puebla, R.A., Garrido, J.J., 2005. Effect of pH on the aggregation of a gray humic acid in colloidal and solid states. Chemosphere 59, 659–667.

Angelico, R., Ceglie, A., He, J.Z., Liu, Y.R., Palumbo, G., Colombo, C., 2014. Particle size, charge and colloidal stability of humic acids coprecipitated with ferrihydrite. Chemosphere 99, 239–247.

Chen, W., Habibul, N., Liu, X.Y., Sheng, G.P., Yu, H.Q., 2015. FTIR and synchronous fluorescence heterospectral two-dimensional correlation analyses on the binding characteristics of copper onto dissolved organic matter. Environ. Sci. Technol. 49, 2052–2058.

Chen, W., Qian, C., Liu, X.Y., Yu, H.Q., 2014. Two-dimensional correlation spectroscopic analysis on the interaction between humic acids and $TiO_2$ nanoparticles. Environ. Sci. Technol. 48, 11119–11126.

Cheng, W.P., Chi, F.H., 2002. A study of coagulation mechanisms of polyferric sulfatereacting with humic acid using a fluorescence-quenching method. Water Res. 36, 4583–4591.

Elkins, K.M., Nelson, D.J., 2002. Spectroscopic approaches to the study of the interaction of aluminum with humic substances. Coord. Chem. Rev. 228, 205–225.

Guan, X.H., Shang, C., Chen, G.H., 2006. ATR-FTIR investigation of the role of phenolic groups in the interaction of some NOM model compounds with aluminum hydroxide. Chemosphere 65, 2074–2081.

He, X.S., Xi, B.D., Zhang, Z.Y., Gao, R.T., Tan, W.B., Cui, D.Y., 2014. Insight into the evolution, redox, and metal binding properties of dissolved organic matter from municipal solid wastes using two-dimensional correlation spectroscopy. Chemosphere 117, 701–707.

Hur, J., Jung, K.Y., Jung, Y.M., 2011. Characterization of spectral responses of humic substances upon UV irradiation using two-dimensional correlation spectroscopy. Water Res. 45, 2965–2974.

Hur, J., Lee, B.M., 2011. Characterization of binding site heterogeneity for copper within dissolved organic matter fractions using two-dimensional correlation fluorescence spectroscopy. Chemosphere 83, 1603–1611.

Hussain, S., Leeuwen, J.V., Chow, C., Beecham, S., Kamruzzaman, M., Wang, D.S., et al., 2013. Removal of organic contaminants from river and reservoir waters by three different aluminum-based metal salts: coagulation adsorption and kinetics studies. Chem. Eng. J. 225, 394–405.

Jin, P.K., Sheng, J.J., Liu, L., Wang, X.C., 2011. Characterization of Al-humic complexation at typical pH. J. Xi'an Univ. Archit. Technol. 43 (2), 215–219.

Li, X.W., Dai, X.H., Takahashi, J., Li, N., Jin, J.W., Dai, L.L., Dong, B., 2014. New insight into chemical changes of dissolved organic matter during anaerobic digestion of dewatered sewage sludge using EEM-PARAFAC and two-dimensional FTIR correlation spectroscopy. Bioresour. Technol. 159, 412–420.

Lin, J.-L., Huang, C., Dempsey, B.A., Hu, J.-Y., 2014. Fate of hydrolyzed Al species in humic acid coagulation. Water Res. 56, 314–324.

Lu, X.Q., Chen, Z.L., Yang, X.H., 1999. Spcetrosopic study of aluminium speciation in removing humic substances by Al coagulation. Water Res. 33 (5), 3271–3280.

Nakashima, K., Xing, S.Y., Gong, Y.K., Miyajima, T., 2008. Characterization of humic acids by two-dimensional correlation fluorescence spectroscopy. J. Mol. Struct. 883-884, 155–159.

Noda, I., 1986. Two-dimensional infrared (2-D IR) spectroscopy of synthetic and biopolymers. Bull. Am. Phys. Soc. 31 (3), 520.

Noda, I., 2012. Close-up view on the inner workings of two-dimensional correlation spectroscopy. Vib. Spectrosc. 60, 146–153.

Noda, I., Ozaki, Y., 2004. Two-dimensional Correlation Spectroscopy. John Wiley & Sons Ltd., West Sussex.

Nordin, J., Persson, P., Laiti, E., Sjoberg, S., 1997. Adsorption of o-phthalate at the water-boehmite ($\gamma$-AlOOH) interface: evidence for two coordination modes. Langmuir 13, 4085–4093.

Piccolo, A., Stevenson, F.J., 1982. Infrared spectra of $Cu^{2+}$, $Pb^{2+}$, and $Ca^{2+}$ complexes of soil humic substances. Geoderma 27, 195–208.

Provenzano, M.R., D'Orazio, V., Jerzykiewicz, M., Senesi, N., 2004. Fluorescence behavior of Zn and Ni complexes of humic acid from different sources. Chemosphere 55, 885–892.

Semmens, M.J., Field, T.K., 1980. Coagulation: experiences in organics removal. J. AWWA 72 (8), 476–485.

Sharpless, C.M., Mcgown, L.B., 1999. Effect of aluminum-induced aggregation on the fluorescence of humic substances. Environ. Sci. Technol. 33, 3264–3270.

Shin, J.Y., Spinette, R.F., O'Melia, C.R., 2008. Stoichiometry of coagulation revisited. Environ. Sci. Technol. 42, 2582–2589.

Wang, W.D., Wang, W., Fan, Q.H., Wang, Y.B., Qiao, Z.X., Wang, X.C., 2014. Effects of UV radiation on humic acid coagulation characteristics in drinking water treatment processes. Chem. Eng. J. 256 (15), 137–143.

Xu, H.C., Yu, G.H., Yang, L.Y., Jiang, H.L., 2013. Combination of two-dimensional correlation spectroscopy and parallel factor analysis to characterize the binding of heavy metals with DOM in lake sediments. J. Hazard. Mater. 263, 412–421.

Yu, G.H., Wu, M.J., Wei, G.R., Luo, Y.H., Ran, W., Wang, B.R., et al., 2012. Binding of organic ligands with Al(III) in dissolved organic matter from soil: implications for soil organic carbon storage. Environ. Sci. Technol. 46, 6102–6109.

Zhou, P., Hui, Y., Bao, H.G., 2005. Competitive complexation of metal ions with humic substances. Chemosphere 58, 1327–1337.

Zhou, M.H., Meng, F.G., 2016. Aluminum-induced changes in properties and fouling propensity of DOM solutions revealed by UV–vis absorbance spectral parameters. Water Res. 93, 153–162.

Zhu, G.C., Yin, J., Zhang, P., Wang, X.F., Fan, G.D., Hua, B., et al., 2014. DOM removal by flocculation process: fluorescence excitation–emission matrix spectroscopy (EEMs) characterization. Desalination 346, 38–45.